Published in final edited form as:
J Phys Chem B. 2013 October 24; 117(42): . doi:10.1021/jp4028113.

Dodine as a Protein Denaturant: The Best of Two Worlds?

Hannah Gelman[†,‡], **Tatyana Perlova**[†,‡], and **Martin Gruebele**[†,§,*]

[†]Department of Physics, Center for the Physics of Living Cells, University of Illinois, Urbana, IL 61801, United States

[§]Department of Chemistry and Center for Biophysics and Computational Biology, University of Illinois, Urbana, Illinois 61801, United States

Abstract

Traditional denaturants such as urea and guanidinium ion unfold proteins in a cooperative "all-or-none" fashion. However, their high working concentration in combination with their strong absorption in the far ultraviolet region make it impossible to measure high quality circular dichroism or infrared spectra, which are commonly used to detect changes in protein secondary structure. On the other hand, detergents such as dodecyl sulfate destabilize native protein conformation at low millimolar concentrations and are UV transparent, but they do denature proteins more gradually than guanidinium or urea. In this work we studied the denaturation properties of the fungicide dodecylguanidinium acetate (dodine), which combines both denaturants into one. We show that dodine unfolds some small proteins at millimolar concentrations, facilitates temperature denaturation, and is transparent enough at its working concentration, unlike guanidinium, to measure full range circular dichroism spectra. Our results also suggest that dodine allows fine-tuning of the protein's unfolded state, unlike traditional "all-or-none" denaturants.

Keywords

fluorescence; tryptophan; lambda repressor; WW domain; membrane protein; guanidine hydrochloride; sodium dodecyl sulfate (SDS)

INTRODUCTION

In vitro studies of protein folding and stability employ a range of techniques to unfold proteins. Chemical denaturants are often used in concert with thermal denaturation to enable the unfolding of thermally stable proteins,[1] to mitigate the aggregation of unfolded states,[2] or to bias proteins towards unfolding in single molecule studies.[3–5]

Current research into the folding mechanism of fast folding proteins is an area of particular interest because the small size and fast kinetics of these proteins allow direct comparison with molecular dynamics simulations. These fast folders are often surprisingly stable for their size, and demand chemical denaturants in concert with other perturbations to reach the unfolded state.

[*]Corresponding author: Tel: 001-217-333-1624, mgruebel@illinois.edu.
[‡]These authors contributed equally.

The authors declare no competing financial interest.

SUPPORTING INFORMATION AVAILABLE

The SI PDF file describes additional measurements (critical micelle concentration, reversibility, and protein concentration dependence) with text, three figures, and one table. This information is available free of charge via the Internet at http://pubs.acs.org/.

In addition, residual structure in the unfolded state is of particular interest because it can have a great influence on folding kinetics, in particular for fast folders whose denatured state is connected to the native state by a small barrier readily crossed by thermal fluctuations. Such studies would also benefit from new chemical denaturants that allow access to a range of unfolded state structures following the cooperative main unfolding transition.

Despite their great utility, the widely employed nitrogen-based chaotropes urea and guanidinium chloride impose some limits on the experimenter's flexibility. They are cooperative "all-or-nothing" agents,[6] limiting the tunability of residual unfolded state protein structure.[2] They absorb strongly in the ultraviolet at useful concentrations (> 1 M), limiting circular dichroism to short sample paths and high protein concentrations. Their strong infrared absorption also hampers other secondary structure-detection techniques, such as amide I band spectroscopy.

Detergents such as sodium dodecyl sulfate (SDS) are alternative agents for chemical denaturation. In contrast to the chaotropes urea and guanidinium, detergents denature proteins very gradually starting at millimolar detergent concentrations. At these low concentrations detergents are transparent below 200 nm, making them compatible with protein circular dichroism.[7] Despite this advantage, detergents are rarely used in globular protein folding studies because unfolding by detergents is often incomplete and uncooperative.[7,8] Instead, they are used in gel electrophoresis to unfold proteins and impart a uniform distribution of negative charge.[9]

In this paper we combine the worlds of small nitrogen-based chaotropes and detergents. Our goal is to obtain a denaturant that combines the useful properties of both families of compounds: a denaturant that (1) induces a cooperative transition at millimolar denaturant concentrations instead of molar concentrations; (2) that lowers substantially the thermal unfolding transition temperature; (3) that allows tunability of the denatured state residual structure once past the cooperative transition; and (4) that is transparent in the ultraviolet and infrared amide I′ regions at its working concentration.

Modifications of the basic guanidinium hydrochloride salts[10,11] and of the basic alkyl chain detergents[12] were tested long ago for enhanced denaturant effectiveness. Walker and co-workers showed in 1983 that adding a long alkyl tail to the nitrogen-based chaotrope biguanide creates a powerful denaturant that unfolds the large protein penicillinase at a concentration less than 1.5 mM, but the compound was never used by other groups or applied to smaller proteins.[11]

We apply an n-alkyl derivative of guanidinium to two small proteins, lambda repressor fragment ($\lambda_{6\text{-}85}$) and WW domain (Figure 1). These proteins are of current interest in fast folding studies because their folding kinetics can be compared directly with molecular dynamics simulations.[13–15] Some of their mutants are thermally very stable, demanding the use of chemical denaturants in experimental studies of the unfolding transition or the unfolded state.[16,17] We use n-dodecylguanidinium acetate (dodine), a readily available commercial fungicide, for our protein denaturation experiments. We also synthesize and test Walker's DebiGuHCl. We show that millimolar dodine induces cooperative unfolding of the α helix bundle $\lambda_{6\text{-}85}$, substantially lowers the protein's melting temperature and allows tuning of residual unfolded state structure after the cooperative transition is complete. However, dodine is less effective on the small β-sheet WW domain. We demonstrate that dodine yields better quality circular dichroism spectra than guanidinium down to 200 nm and that it is more transparent than guanidinium in the amide I′ infrared spectrum at their respective working concentrations. We also show that DebiGuHCl is likely to have similar properties as dodine for small proteins.

The family of n-alkyl guanidinium derivatives promises to be a useful tool for the study of small, rapidly folding proteins as it maintains a cooperative melting transition, allows tuning of the denatured ensemble, and is more transparent than conventional denaturants in the far UV and amide I′ spectral regions.

METHODS

Temperature- and denaturant-unfolding studies of the Tyr22Trp/Gln33Tyr/Gly46,48Ala mutant of $\lambda_{6\text{-}85}$[18] and of the Fip35 WW-domain[19] were conducted using commercially available guanidinium chloride and n-dodecylguanidinium acetate (dodine) (both Sigma-Aldrich, St. Louis, MO). Protein conformation upon thermal and chemical denaturation was monitored by circular dichroism (sensitive to overall secondary structure) and tryptophan fluorescence. The latter is most sensitive to a tertiary structure interaction between Tryptophan 22 in helix 1 and tyrosine 33 in helix 2 of $\lambda_{6\text{-}85}$.[18] Guanidinium titrations were performed in phosphate buffer (see below). Dodine titrations were performed in aqueous solution because the solubility of the commercially available acetate salt is low in phosphate buffer, but reaches approximately 5 mM in water. 100-200 mM dodine acetate was pre-dissolved in small amounts of ethanol and then diluted down to experimental concentrations.

Protein expression and purification

Both $\lambda_{6\text{-}85}$ and WW domain were expressed in BL-21 CodonPlus DE-3 RIPL cells (Agilent Technologies, Santa Clara, CA) according to published protocols.[19,20] Cells were grown at 37 °C in LB broth (Fisher Scientific, Pittsburgh, PA) in the presence of 100 mg/L of Ampicillin (Fisher Scientific, Pittsburgh, PA) to an OD_{600} of 0.6 to 1, and induced overnight with 1 mM isopropyl β-D-thiogalactopyranoside (IPTG) (Inalco, Milano, Italy) at 25 °C. Cells were harvested by centrifugation at 5,000 rpm for 20 minutes and resuspended in lysis buffer. Cells were lysed *via* sonication and the soluble fraction was isolated by centrifugation at 10,000 rpm for 20 minutes. Each protein was isolated by affinity chromatography (see below). Affinity tags were removed by Thrombin cleavage, according to the manufacturer's protocol (EMD Millipore, Billerica, MA). Thrombin and protein were separated either by isolating biotinylated thrombin on a streptavidin agarose column (EMD Millipore, Billerica, MA) or *via* size exclusion filtration. Cleaved proteins were lyophilized overnight and stored at −80 °C until re-suspension. For measurements, proteins were dissolved into 20 mM phosphate buffer, pH = 7.0–7.5 or into sterile MilliQ water (EMD Millipore, Billerica, MA).

λ was expressed from a pET-15b (EMD Millipore, Billerica, MA) vector encoding an N-terminal hexahistidine tag and a thrombin recognition sequence. The lysis buffer was 150 mM NaCl, 50 mM Na_2HPO_4, 10 mM imidazole (Sigma-Aldrich, St. Louis, MO); pH 8.0. Protein was isolated using a nickel charged Ni-NTA column according to the manufacturer's protocol (EMD Millipore, Billerica, MA).

The gene for Fip35 WW-domain was cloned with an N-terminal glutathione S-transferase (GST) tag (sequence the same as in the pGEX vectors, GE Healthcare Biosciences, Pittsburgh, PA) and thrombin recognition sequence into the pDream vector (Genscript, Piscataway, NJ). Cells were lysed in buffer containing 10 mM Na_2HPO_4, pH 7.0 and cell extract was purified on a glutathione-agarose column according to the manufacturer's protocol (Genscript, Piscataway, NJ).

Spectroscopic probes of denaturation

Circular dichroism was measured using a Jasco spectrometer with Peltier temperature control (Jasco Inc, Easton, MD). Unless otherwise noted, all spectra were recorded from 250

– 200 nm at a scan rate of 50 nm/min with 1 nm resolution. Presented spectra are an average of 5–10 accumulations. Chemical denaturant titrations were conducted at room temperature (20–25 °C). Measurements of $\lambda_{6\text{-}85}$ were done using a 1 mm path length cuvette and WW-domain measurements were done in a 1 cm cuvette. Due to the high absorbance of guanidinium and the small circular dichroism signal of WW domain, the guanidinium melt of WW domain was done at 25 μM protein in a 2 mm path length cuvette. We have seen no concentration dependence in the WW domain melts with guanidinium for concentrations ranging from 10–100 μM (data not shown). Unless otherwise noted, protein concentrations in other experiments were approximately 10 μM.

Tryptophan fluorescence measurements were taken on a Cary Eclipse spectrophotometer (Agilent Technologies, Santa Clara, CA) equipped with Peltier temperature control. The excitation wavelength was 280 nm and emission spectra were collected from 290–450 nm. Samples were measured in 140 μL or 400 μL cuvettes and, unless otherwise noted, at 10 μM concentration.

Fourier transform infrared (FTIR) spectra of guanidium and dodine were taken using a Nicolet Magna IR spectrometer (Fisher Scientific, Pittsburgh, PA). 15 μL of sample (dissolved in 99% deuterium oxide to avoid the strong absorption of water in the amide I′ region) was placed between calcium fluoride windows and spectra were taken from 4000–600 cm^{-1}.

Data analysis

Data was analyzed using Matlab (Mathworks Inc., Natick, MA) and Igor Pro (Wavemetrics Inc, Lake Oswego, OR). Circular dichroism spectra were analyzed by the evolution of the circular dichroism signal at representative wavelengths (222 nm for $\lambda_{6\text{-}85}$, 227 nm for WW-domain) under thermal or chemical denaturation. A scattering baseline was subtracted (CD at 245 nm, where the far-UV CD signal due to secondary structure approached zero for proteins in water or phosphate buffer).

$\lambda_{6\text{-}85}$ tryptophan fluorescence was analyzed by tracking the shift in emission peak wavelength as a function of temperature or denaturant concentration. The peak wavelength was located by fitting the emission intensity I as a function of wavelength λ from 310 – 380 nm to a Gaussian function, where the center wavelength λ_0 represents the fitted peak wavelength:

$$I(\lambda)=y_0+A\exp(-(\lambda-\lambda_0)^2/2\sigma^2) \quad (1)$$

WW-domain tryptophan fluorescence does not undergo a significant wavelength shift during protein denaturation. Consistent with previously published methods,[17,19] WW unfolding was analyzed by tracking the decrease in fluorescence intensity during denaturation. All spectra were normalized by the maximum intensity observed during the melt and the relative peak intensity is reported as the normalized intensity.

Melting temperatures (T_m) and denaturation midpoints (C_m) were calculated using a two-state thermodynamic fit. Native and denatured state baselines were assumed to be linear in the perturbing variable X (either temperature or concentration) so that the signal could be modeled as

$$S_i=m_i\,(X-X_m)+b_i \quad (2)$$

where *i* denotes either native or denatured. The total signal is then modeled as

$$S(X)=(S_N K_{eq}+S_D)/(1+K_{eq}),\ \text{where}\ K_{eq}=\exp(-\Delta G/k_B T)\ \text{and}\ \Delta G \approx \delta g_1(X-X_m) \quad (3)$$

and fits to this equation allow us to extract a midpoint value (X_m) for the perturbation of interest. Models with more floating parameters (e.g. a heat capacity model for unfolding) did not provide X_m values with smaller uncertainties.

Synthesis of n-decylbiguanidinium chloride

DebiGu HCl was synthesized following the procedure described by Mitchinson, *et al.*[11] To synthesize n-decylammonium chloride, 10 ml of ether (Sigma Aldrich, St. Louis, MO) was added to 10 ml of n-decylamine (Sigma Aldrich, St. Louis, MO) in a well-stirred round bottom flask. Then 30 ml of 2M HCl in ether (Fisher, Pittsburgh, PA) was slowly added to the flask with a syringe. The white solid was filtered off and dried under vacuum. The yield was 8.7 g. The chemical identity of the product was confirmed by ESI mass spectrometry. n-decylammonium chloride (2g) was then ground in a mortar with dicyandiamide (0.84g) (Sigma Aldrich, St. Louis, MO) and heated up to 150 °C under nitrogen in a round bottom sealed flask on a silicon oil bath. The resulting melt was poured into chilled acetone and stirred for about 30 min. The cooled mix was poured into ether, filtered and dried under vacuum. The procedure yielded 1.14 g of wax-like material. According to ESI mass spectrometry the main components of the resulting mix were the desired n-decylbiguanide hydrochloride and impurities of n-decylguanidinium chloride and unreacted n-decylammonium chloride. Denaturation efficacy of this product was tested without further purification, starting with a *ca.* 0.5 M stock solution in 20 mM K_2PO_4, pH 7.0.

RESULTS

We compared the effect of dodine, which has a long alkyl chain connected to the guanidinium group, to the effect of the standard denaturant guanidinium chloride on protein stability. Unfolding was detected by circular dichroism (sensitive to secondary structure) and fluorescence (sensitive to tertiary structure near the tryptophan probe). Denaturant-induced unfolding was also combined with thermal unfolding. We chose two structurally very different small proteins, the five helix bundle $\lambda_{6\text{-}85}$, and the triple stranded β-sheet WW domain (Figure 1), allowing us to assess the effect of protein secondary structure on dodine's effectiveness as a denaturant. The Tyr22Trp/Gln33Tyr/Gly46,48Ala mutant of $\lambda_{6\text{-}85}$ exhibits high thermal stability ($T_m \approx 70$ °C) and has been shown to fold downhill under favorable solvent conditions.[21–23] The Fip35 variant of WW domain used here is a small (34 residue) β hairpin that also exhibits high stability ($T_m \approx 78$ °C) and incipient downhill folding.[18,19] Like $\lambda_{6\text{-}85}$, WW domain is extensively used as a model protein for both experimental and computational folding studies.[17]

Critical micelle concentration of dodine

Although dodine, with its guanidinium headgroup, is not a conventional detergent like SDS, we are interested in its denaturation properties under conditions resembling ordinary chaotropes, in the absence of micelle formation. The critical micelle concentration (CMC) of dodine was measured by the pyrene titration method,[25] and is 8.7±1.9 mM (see Figure S1 in Supplementary Information). In all subsequent experiments, we kept the working range of dodine concentrations substantially below the CMC.

Dodine vs. guanidine cooperative unfolding transitions

Initial experiments determined the cooperative denaturation midpoints (C_m) of $\lambda_{6\text{-}85}$ in guanidinium and dodine. We used fluorescence to monitor the shift in the peak emission wavelength as a function of denaturant concentration (Figure 2). The measured guanidinium C_m is 2.7 M, while the dodine C_m ranges from 1.7 – 2.4 mM, depending on protein concentration. We observe that denaturation by guanidinium results in a larger peak shift (331 – 356 nm) than denaturation by dodine (330 – 340 nm). Denaturation by titration with either compound is reversible (see SI for discussion of reversibility) The concentration dependence of the dodine C_m is characteristic of detergent denaturation,[7,26] an indication that both components of the dodine compound (the guanidinium head group and the alkyl chain) contribute to the cooperative unfolding transition. This is further supported by the observation that the cooperative transition in the dodine denaturation curve lies at more than 1000-fold lower concentration than for guanidinium without an alkyl chain attached.

Corresponding titrations detected by circular dichroism show denaturation midpoints at 3 M guanidinium and 1.6 mM dodine (data not shown). At the midpoint, the ellipticity in dodine decreases by only 10%, compared to 75% in guanidinium (in 1 mM dodine and 2.5 M guanidinium, the decreases are 9% and 58%, respectively).

Thus dodine fulfills the first requirement we enumerated in the introduction: titration with dodine results in a cooperative $\lambda_{6\text{-}85}$ unfolding transition at concentrations ~1000 times lower than those required for guanidinium induced unfolding. However, loss of secondary structure immediately after the transition is much more complete in guanidinium than in dodine.

Millimolar dodine substantially lowers the $\lambda_{6\text{-}85}$ melting temperature

We are particularly interested in how the hybrid denaturant assists thermal denaturation of small proteins. To compare dodine with guanidinium, we performed melts of $\lambda_{6\text{-}85}$ in three chemical environments – in aqueous solution without denaturant, in the presence of 2.5 M guanidinium and in the presence of 0.5–1.65 mM dodine. The process of denaturation was monitored by fluorescence and circular dichroism spectroscopy (Figure 3). Melting temperatures T_m in the different environments are summarized in Table 1.

Fig. 3A highlights an interesting property of dodine-assisted thermal denaturation. At low dodine concentrations (<1–1.5 mM), dodine reduces T_m by up to 15 °C, and the transition remains cooperative (with reduced slope at the midpoint). At higher dodine concentrations (>1.5–2 mM), the thermal denaturation curve has two distinct phases: a smaller cooperative transition is followed by a more gradual transition resembling ‘linear’ detergent behavior. At intermediate dodine concentrations, the relative amplitude of the cooperative and linear phases, as well as T_m, also depend on the protein concentration (Figure S2, Supplementary Information). This is to be expected based on the protein concentration dependence discussed above for dodine-only denaturation (Figure 2).

Dodine satisfies the second criterion outlined in the introduction. The fluorescence data (Figure 3A) show that the cooperative part of the thermal unfolding transition of $\lambda_{6\text{-}8}$ is lowered by about 35 °C in the presence of 1.65 mM dodine. In contrast, 2.5 M guanidinium is required to achieve similar destabilization of $\lambda_{6\text{-}85}$. In 1.65 mM dodine the protein reaches a less extensively denatured state right after the cooperative transition, which continues to lose structure gradually to approach full denaturation by 95 °C. Thus residual structure of the unfolded protein can be tuned over a wide range with the right choice of protein and dodine concentrations. This third criterion mentioned in the introduction is potentially a very useful feature for protein refolding studies. Refolding kinetics are known to depend on residual unfolded state structure,[27] which could be systematically tuned with dodine.

Control experiments (Figure 3B) show that 1 mM SDS alone, or in combination with 1 mM guanidinium, produced no significant unfolding of tertiary structure over the entire temperature range, nor did 1 mM guanidinium alone shift the thermal denaturation midpoint T_m. Although it has been reported that low concentrations of SDS can induce cooperative conformational transitions,[7,28] this data shows that the effect of dodine is fundamentally different from the effect of its two constituent parts at the same concentration.

CD data (Figure 3C) show only a gradual loss of secondary structure and no cooperative transition in dodine. As with the fluorescence data, the protein eventually approaches full loss of secondary structure at high temperature. Dodine's smaller effect on secondary structure stability in a thermal melt is consistent with its smaller effect on secondary structure in isothermal titrations. The Discussion section goes over the mechanistic implications of the fluorescence/CD difference and cooperative/linear unfolding phases observed when dodine is used as a protein denaturant.

Dodine is transparent in the ultraviolet and infrared amide I′ regions at its working concentration

One of the disadvantages of guanidinium is its high absorbance in the ultraviolet region at its working concentration, making it impossible to measure high quality circular dichroism spectra at short wavelengths (Figure 4A). In contrast, dodine at its working concentration allows the collection of smooth circular dichroism spectra down to 200 nm (Figure 4B).

This advantage is due to the lower working concentration of dodine, not lower absorbance in absolute terms. Measurements of dodine and guanidinium absorbance were conducted in spectroscopic grade ethanol (Acros Organics) to allow measurement of dodine at higher concentrations than are soluble in water. These measurements showed that dodine and guanidinum have similar absorbance spectral shapes, but the absorption coefficient of dodine is approximately ten times higher on a molar basis than for guanidinium. The 1000 times smaller dodine concentration needed for denaturation experiments more than compensates for its higher molar absorption coefficient (absorption spectra in aqueous solution at 1 M GuHCl, 1 mM dodine in the inset of Figure 4B).

Figure 4C compares the infrared spectrum of dodine acetate and GuHCl. 1 mM dodine, close to the actual working concentration used in our experiments, does not absorb enough in the amide I′ region to provide a reliable signal (red trace), but we can infer from the 10 mM results (blue trace) that its peak absorbance between 1400 and 1700 cm^{-1} will be about 50 times less than that of 1 M GuHCl. Due to its low working concentration, dodine has a marked advantage in infrared monitoring of protein denaturation, in addition to its advantage in the ultraviolet below 250 nm. Dodine's transparency in the amide I′ region could be of interest for pressure denaturation experiments, where infrared spectroscopy is often the only option for secondary structure determination because strain on cell windows distorts the circular dichroism signal.

< 2 mM dodine only slightly destabilizes WW domain

Despite their similar thermal stabilities, FiP35 WW domain is much more resistant to chemical denaturation than $\lambda_{6\text{-}85}$: unfolding is incomplete even in 5.5 M guanidinium when assessed by circular dichroism or fluorescence. No signs of denaturation are observed at room temperature at dodine concentrations up to 2 mM (data not shown).

However, dodine does have an effect on the thermal denaturation of WW domain. We examined it without denaturant, in 2 M guanidinium, and in 1 mM dodine by both fluorescence and circular dichroism (Figure 5). We tracked the change in fluorescence intensity, measured relative to the maximum intensity observed throughout the melt.[17,19]

(WW does not have a wavelength shift.) To monitor unfolding by circular dichroism, we tracked the circular dichroism signal at 227 nm.[19] The addition of 2 M guanidinium lowers the melting temperature T_m by ≈ 20 °C. 1 mM dodine lowers T_m only by ≈ 5 °C, in contrast to the large (≈ 25 °C) destabilization observed for $\lambda_{6\text{-}85}$ in 1.65 mM dodine (Figure 3). In addition, we observe that the WW domain transition in dodine does not exhibit the gradual unfolding tail seen in the $\lambda_{6\text{-}85}$ melts. Quite the opposite, the WW domain transition in most cooperative in dodine (δg_1 in table 1 is largest in dodine), whereas guanidium melts of WW domain show a broad and gradual transition monitored by both circular dichroism and fluorescence.

DebiGuHCl is likely to have similar properties as dodine

DebiGu is the hybrid denaturant previously investigated by Walker and coworkers in the context of a large, slow folding protein.[11] We prepared DebiGuHCl (with some impurities) as described in Methods. Figure 6 compares fluorescence-detected melts of $\lambda_{6\text{-}85}$ in the presence of 2 M guanidinium, 1 mM dodine, and 5 mM DebiGu. The denaturation midpoint $T_m \approx 54$ °C in 5 mM DebiGu is roughly equivalent to 2 M guanidinium. Like the dodine denaturation curves, the post-transition baseline in the presence of DebiGu has an upward slope. In this case, however, the peak wavelength shift is much more pronounced, even when compared to the shift in pure buffer or with guanidinium. This significant shift in tryptophan fluorescence may be due to interactions between the biguanine headgroup and the exposed tryptophan indole ring that alter the indole groups' emission spectrum. Additionally, DebiGu has higher ultraviolet absorption than dodine (data not shown); this may be due to the biguanine headgroup.

In contrast to dodine (acetate salt), we had no solubility problems with DebiGuHCl in phosphate buffer up to 0.5 M denaturant concentration. We believe that the counterion mixture is responsible, in which case dodine as the chloride instead of the acetate salt may allow a wider range of denaturant concentrations to be used.

Discussion

Our results demonstrate that dodine can be used as a hybrid denaturant for some small, fast folding proteins. By linking together a guanidine headgroup and an alkyl tail, it combines useful properties of small chaotropes and long-chain surfactants. Dodine preserves the cooperative transition of the small chaotropes, but at 1000x smaller concentration. The cooperative transition produces a less extensively denatured state, whose residual secondary and tertiary structure can be tuned with temperature. In the presence of dodine, raising the temperature past the cooperative transition temperature continues to gradually reduce residual structure in the unfolded state.

Dodine likely destabilizes tertiary structure first

Taken together, the circular dichroism and fluorescence data suggest that dodine acts by destabilizing tertiary structure first, leaving secondary structure open to further perturbation after the cooperative transition is complete. Tertiary structure sensitive fluorescence monitored during isothermal titrations shows a cooperative transition accounting for ~1/3 of the guanidinium titration peak shift, while secondary structure sensitive circular dichroism measurements show only 10% loss of signal over the same range of dodine concentrations (compared with 78% loss of signal for guanidinium). This mechanism also helps explain features of the dodine assisted thermal melts of $\lambda_{6\text{-}85}$. Fluorescence melts show a destabilized transition accounting for ~1/3 of the guanidinium assisted melt peak shift, while circular dichroism melts show a gradual loss of secondary structure. The linear unfolded state baseline apparent in both dodine and DebiGu fluorescence melts are consistent with

gradual loss of residual secondary and tertiary structure as the temperature is increased beyond the cooperative melting transition.

Interestingly, Otzen and Oliveberg found that much higher concentrations of SDS than the working concentration of dodine (>200 mM) similarly disrupt tertiary structure while leaving some secondary structure intact.[29] They attribute this mechanism to the types of micelles formed at high SDS concentrations. In this work we are using concentrations of dodine well below its critical micelle concentration (see Supplementary Information). However, Otzen and Oliveberg suggest that the detergent micelles act as "denaturants" in the solution, rather than binding to well defined sites on the protein.[30] Perhaps the addition of a denaturant headgroup in dodine allows this mechanism to become active at sub-micellar concentrations.

Experimentalists need a transparent denaturant

Dodine is of particular interest when tuning of secondary structure, e.g. by temperature or pressure denaturation, is desired. Its smaller absorption coefficient in the 200–250 nm range at the working concentration leads to cleaner circular dichroism spectra of proteins. Based on Figure 4C, the same is likely true for amide I′ band infrared spectra. It may be that dodine is the only viable denaturant for secondary structure sensitive pressure denaturation experiments (i.e. *via* FTIR) because even GuDCl strongly obscures the amide I′ band of proteins at the working concentrations (>1 M) required to achieve the onset of denaturation.

Dodine's effectiveness is protein-dependent

Dodine behaves very differently for two proteins with fundamentally different structure, the five helix bundle $\lambda_{6\text{-}85}$, and the triple stranded β-sheet Fip35 WW domain. Its effectiveness in assisting WW domain thermal denaturation is about 4–5 times less than for $\lambda_{6\text{-}85}$. In addition, dodine increases the cooperativity of WW domain unfolding relative to aqueous solution or GuHCl solution, whereas it produces the aforementioned gradual loss of denatured state structure in $\lambda_{6\text{-}85}$. This could be an indication that dodine interacts more site-specifically with the backbone or sidechains of WW domain. A possible reason could be different exposure of protein-protein H-bonds in helical *vs.* sheet secondary structure. Detergents are also significantly more effective at unfolding α helices than *β* sheets.[8] Thus, dodine's dependence on secondary structure is likely due to the detergent character of the long alkyl tail connected to the guanidine group. The dependence of dodine C_m on protein concentration is also consistent with its detergent character,[7,26] as sub-micellar detergents are thought to bind to limited numbers of sites on each protein, thereby limiting their effectiveness at concentrations below or near the K_d of the detergent-binding site interaction.

Despite the similarities between dodine and detergent interactions with proteins, however, there are significant differences. As we have seen, 1 mM SDS does not destabilize the cooperative unfolding of $\lambda_{6\text{-}85}$, but rather makes unfolding extremely gradual. This makes SDS less useful than dodine for temperature- or pressure-jump experiments, which depend on perturbing a system across a cooperative transition to produce a large signal change.

n-alkyl guanidinium derivitives are likely to share similar properities

Compounds of related structure, such as DebiGu, are likely to have similar properties as dodine. Walker and co-workers tested propyl- and hexyl- biguanide HCl as well as DebiGu and found that the effectivness of the denaturant on penicillinase increased with the alkyl chain length.[11] An advantage noted for the synthesized DebiGu chloride over the commercial dodine acetate is the improved solubility in aqueous salt buffers of the former. We propose that this difference is due to a salting-out effect of acetate on dodine by promotion of micelle formation. Indeed, concentrations above 3 mM dodine in water, or

temperatures below 35 °C (see Figure 5B, red data points) produce scattering in the solution due to turbidity. Such an effect is not observed in the DebiGu chloride salt up to 500 mM concentration, or in alcohol solutions of dodine, suggesting chloride as the most inocuous counterion for future studies.

Supplementary Material

Refer to Web version on PubMed Central for supplementary material.

Acknowledgments

Financial support was provided by the National Science Foundation Center for the Physics in Living Cells, Grant 0822613. H. G. was also supported by the National Institutes of Health grant R01-GM093318. We thank Dustin Gross and Lea Nienhaus for help with DebiGu synthesis, Anna Jean Wirth and Maxim Prigozhin for assistance with $\lambda_{6\text{-}85}$ and WW domain expression, and Kevin Teng for help with measurements of dodine CMC. FTIR spectroscopy was performed in the laboratory of Professor Prashant Jain (UIUC).

Abbreviations

GuHCl, Guanidine hydrochloride	guanidinium chloride
dodine	n-dodecylguanidinium
DebiGu	n-decylbiguanidinium

References

1. England JL, Haran G. Role of Solvation Effects in Protein Denaturation: From Thermodynamics to Single Molecules and Back. Ann Rev Phys Chem. 2011; 62:257–277. [PubMed: 21219136]
2. Dill KA, Shortle D. Denatured States of Proteins. Ann Rev Biochem. 1991; 60:795–825. [PubMed: 1883209]
3. Rhoades E, Cohen M, Schuler B, Haran G. Two-State Folding Observed in Individual Protein Molecules. J Am Chem Soc. 2004; 126:14686–14687. [PubMed: 15535670]
4. Huang F, Ying L, Fersht AR. Direct Observation of Barrier-Limited Folding of Bbl by Single Molecule Fluorescence Resonance Energy Transfer. Proc Natl Acad Sci. 2009; 106:123–127.
5. DeCamp SJ, Naganathan AN, Waldauer SA, Bakajin O, Lapidus LJ. Direct Observation of Downhill Folding of Lambda-Repressor in a Microfluidic Mixer. Biophys J. 2009; 97:1772–1777. [PubMed: 19751683]
6. Greene RF, Pace CN. Urea and Guanidine Hydrochloride Denaturation of Ribonuclease, Lysozyme, Alpha-Chymotrypsin, and Beta-Lactoglobulin. J Biol Chem. 1974; 249:5388–5393. [PubMed: 4416801]
7. Otzen D. Protein-Surfactant Interactions: A Tale of Many States. Biochim Biophys Acta. 2011; 1814:562–591. [PubMed: 21397738]
8. Nielsen MM, Andersen KK, Westh P, Otzen DE. Unfolding of Beta- Sheet Proteins in Sds. Biophys J. 2007; 92:3674–3685. [PubMed: 17351005]
9. Garavito RM, Ferguson-Miller S. Detergents as Tools in Membrane Biochemistry. J Biol Chem. 2001; 276:32403–32406. [PubMed: 11432878]
10. Castellino FJ, Barker R. The Denaturing Effectiveness of Guanidinium, Carbamoylguanidinium, and Guanylguanidinium Salts. Biochemistry. 1968; 7:4135–4138. [PubMed: 5749177]
11. Mitchinson C, Pain R, Vinson J, Walker T. The Relative Effectiveness of Guanidinium and Some Biguanide Salts as Denaturants. Biochim Biophys Acta. 1983; 743:31–36. [PubMed: 6600627]
12. Decker RV, Foster JF. The Interaction of Bovine Plasma Albumin with Detergent Anions. Stoichiometry and Mechanism of Binding of Alkylbenzenesulfonates. Biochemistry. 1966; 5:1242–1254. [PubMed: 5958200]

13. Snow CD, Nguyen H, Pande VS, Gruebele M. Absolute Comparison of Simulated and Experimental Protein-Folding Dynamics. Nature. 2002; 420:102–106. [PubMed: 12422224]
14. Cho SS, Weinkam P, Wolynes PG. Origins of Barriers and Barrierless Folding in BBL. Proc Natl Acad Sci. 2008; 105:118–123. [PubMed: 18172203]
15. Lindorff-Larsen K, Piana S, Dror RO, Shaw DE. How Fast-Folding Proteins Fold. Science. 2011; 334:517–520. [PubMed: 22034434]
16. Prigozhin MB, Liu Y, Wirth AJ, Kapoor S, Winter R, Schulten K, Gruebele M. Misplaced Helix Slows Down Ultrafast Pressure-Jump Protein Folding. Proc Natl Acad Sci. 2013; 110:8087–8092. [PubMed: 23620522]
17. Piana S, Sarkar K, Lindorff-Larsen K, Guo M, Gruebele M, Shaw DE. Computational Design and Experimental Testing of the Fastest Folding [Beta]-Sheet Protein. J Mol Biol. 2011; 405:43–48. [PubMed: 20974152]
18. Liu F, Du D, Fuller AA, Davoren JE, Wipf P, Kelly JW, Gruebele M. An Experimental Survey of the Transition between Two State and Downhill Protein Folding Scenarios. Proc Natl Acad Sci. 2008; 105:2369–2374. [PubMed: 18268349]
19. Liu F, Nakaema M, Gruebele M. The Transition State Transit Time of WW Domain Folding is Controlled by Energy Landscape Roughness. J Chem Phys. 2009; 131:195101. [PubMed: 19929078]
20. Prigozhin MB, Sarkar K, Law D, Swope WC, Gruebele M, Pitera J. Reducing Lambda Repressor to the Core. J Phys Chem B. 2011; 115:10648–10653.
21. Prigozhin MB, Gruebele M. The Fast and the Slow: Folding and Trapping of Lambda(6-85). J Am Chem Soc. 2011; 133:19338–19341. [PubMed: 22066714]
22. Yang WY, Gruebele M. Folding at the Speed Limit. Nature. 2003; 423:193–197. [PubMed: 12736690]
23. Liu F, Gruebele M. Tuning Lambda(6-85) Towards Downhill Folding at Its Melting Temperature. J Mol Biol. 2007; 370:574–584. [PubMed: 17532338]
24. Liu F, Gao YG, Gruebele M. A Survery of Lambda Repressor Fragments from Two-State to Downhill Folding. J Mol Biol. 2010; 397:789–798. [PubMed: 20138892]
25. Hunter, RJ. Foundations of Colloid Science. Vol. 1. Clarendon Press; Oxford, UK: 1987.
26. Tanford C. Protein Denaturation. Adv Prot Chem. 1968; 23:121–282.
27. Dyer RB, Maness SJ, Franzen S, Fesinmeyer RM, Olsen KA, Andersen NH. Hairpin Folding Dynamics: The Cold-Denatured State Is Predisposed for Rapid Refolding. Biochemistry. 2005; 44:10406–10413. [PubMed: 16042418]
28. Malmendal A, Underhaug J, Otzen DE, Nielsen NC. Fast Mapping of Global Protein Folding States by Multivariate NMR: A Gps for Proteins. PLoS One. 2010; 5:e10262. [PubMed: 20421996]
29. Otzen DE, Oliveberg M. Conformational Plasticity in Folding of the Split •-•-• Protein S6: Evidence for Burst-Phase Disruption of the Native State. J Mol Biol. 2002; 317:613–627. [PubMed: 11955013]
30. Otzen DE. Protein Unfolding in Detergents: Effect of Micelle Structure, Ionic Strength, pH, and Temperature. Biophys J. 2002; 83:2219–2230. [PubMed: 12324439]

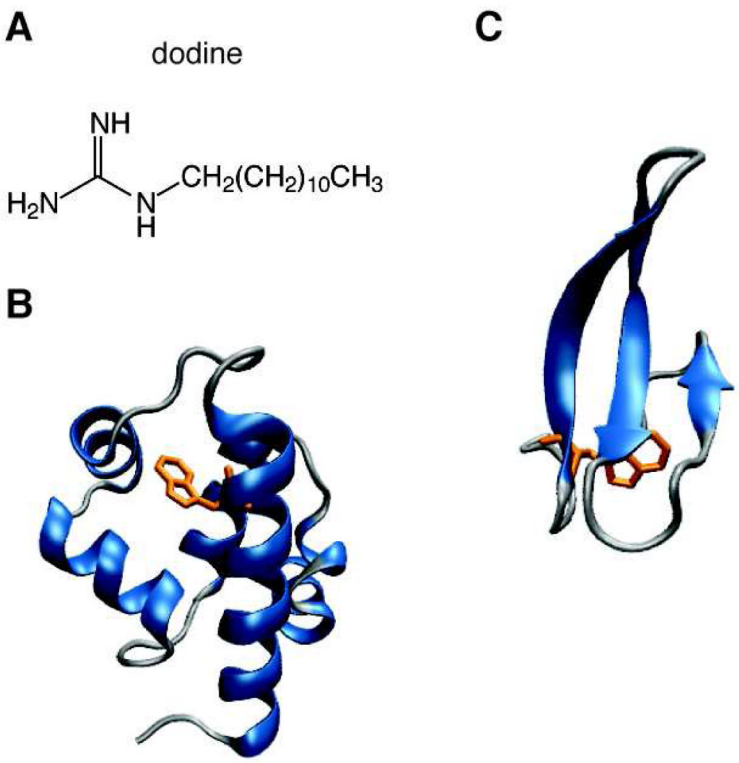

Figure 1.

(A) Structure of dodine (here: neutral form instead of acetate salt). **(B)** Ribbon structure of the $\lambda_{6\text{-}86}$ mutant Tyr22Trp/Gln33Tyr/Gly46,48Ala based on the X-ray crystal structure 3KZ3.[24] **(C)** Ribbon structure of Fip35 WW domain, based on the NMR structure.[18] Highlighted in orange is the Trp residue monitored in fluorescence experiments.

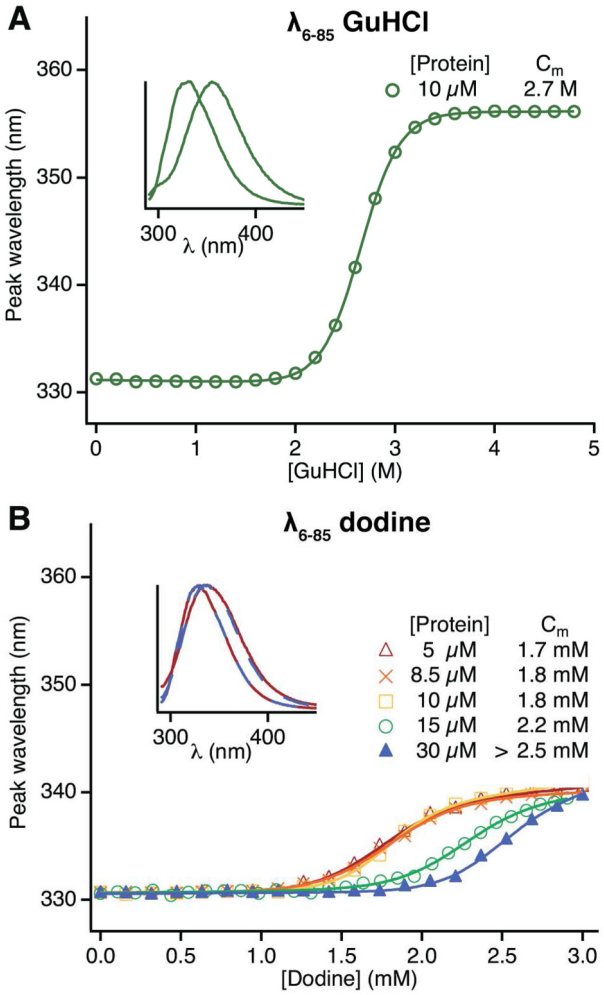

Figure 2.

Fluorescence denaturation curves of $\lambda_{6\text{-}85}$ measured in guanidinium (A) and dodine (B). Insets show the emission spectra at 0 M denaturant and at the maximum denaturant concentration. (A) The concentration midpoint (C_m) in guanidinium is 2.7 M. The total peak shift in the emission spectra is 25 nm. (B) demonstrates that denaturation *via* dodine is protein concentration-dependent. The inset shows that the initial and final spectra at 5 μM (red) and 30 μM (blue) overlap. Total peak shift for all concentrations is 10 nm. Data in (A) from ref. 21.

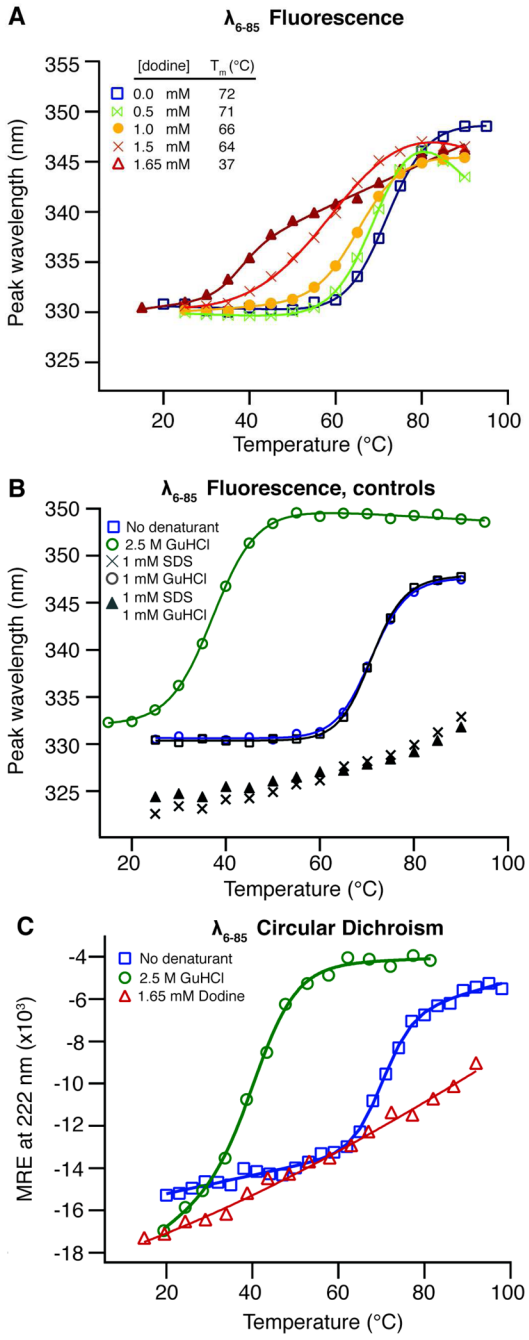

Figure 3.

$\lambda_{6\text{-}85}$ thermal denaturation monitored without denaturant (blue), in 2.5 M guanidinium, and in dodine. Circles, squares and triangles represent experimental points; solid lines are thermodynamic fits to the data. Denaturation midpoints resulting from the fits T_m are shown in Table 1. (A) Peak wavelength as a function of temperature monitored by fluorescence. 0.5 mM to 1.65 mM traces show how the effect of dodine on thermal stability changes as the concentration of dodine is increased. (B) Controls: mM concentrations of guanidinium or SDS, or combinations thereof, do not produce a lower temperature cooperative transition like dodine. No denaturant (blue) and 2.5 M GuHCl (green) traces are presented for

comparison (C) Mean residue ellipticity at 222 nm versus temperature monitored by circular dichroism spectroscopy.

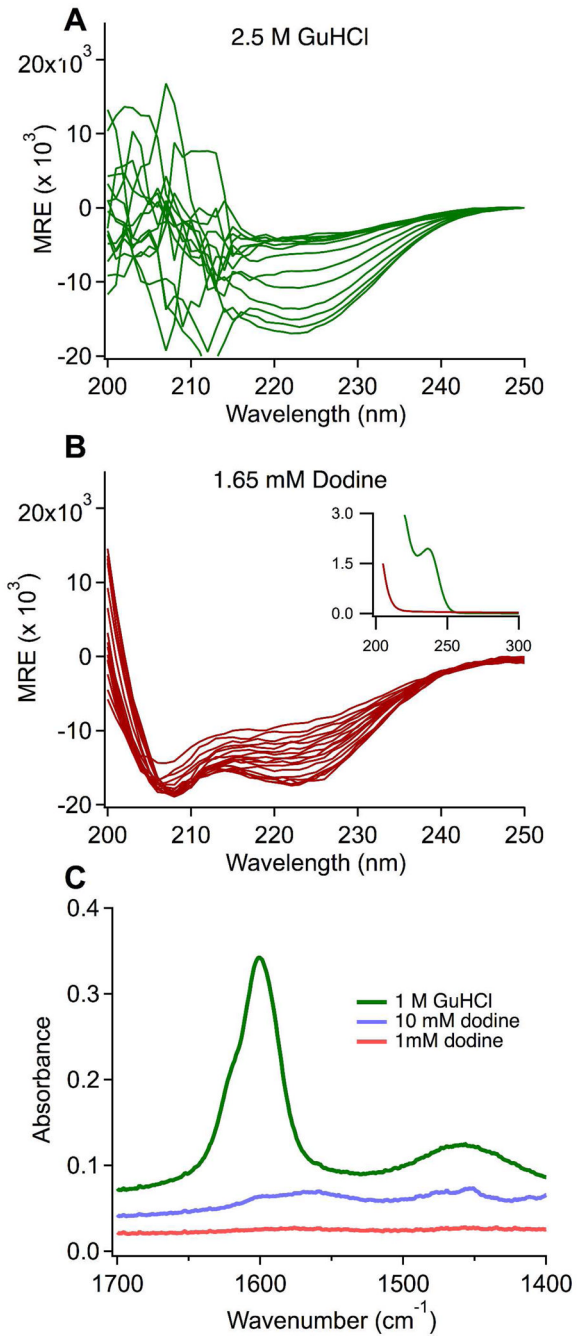

Figure 4.

Circular dichroism spectra of $\lambda_{6\text{-}85}$ undergoing thermal denaturation in the presence of (A) 2.5 M guanidinium (green) and (B) 1.65 mM dodine (red). The inset in panel (B) compares aqueous ultraviolet absorption of dodine (1 mM) and GuHCl (1 M). (C) Infrared spectra near the amide 1′ region of GuHCl (1 M) and dodine (10 mM and 1 mM acetate salt). Traces are offset for clarity. At their working concentrations (1000x lower for dodine), the ratio of maximum absorption for dodine:GuHCl is 1:50.

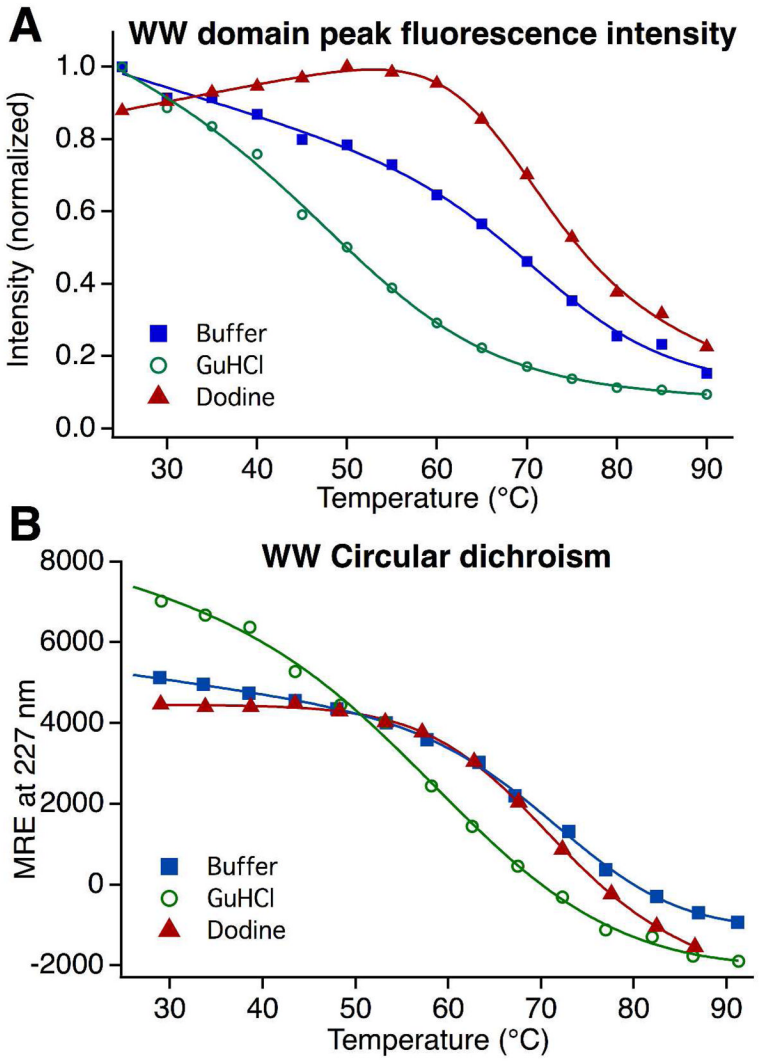

Figure 5.

Fluorescence (A) and circular dichroism melts (B) of WW domain in the absence of denaturant (solid blue squares), in 2 M Guanidinium (green circles), and in 1 mM dodine (red triangles). 2 M guanidinium has an effect on WW domain ($\Delta T_m \approx -20$ °C) comparable to its effect on $\lambda_{6\text{-}85}$ in Figure 3, whereas dodine has a significantly smaller effect ($\Delta T_m \approx -5$ °C), but increases cooperativity more (δg_1 in Table 1).

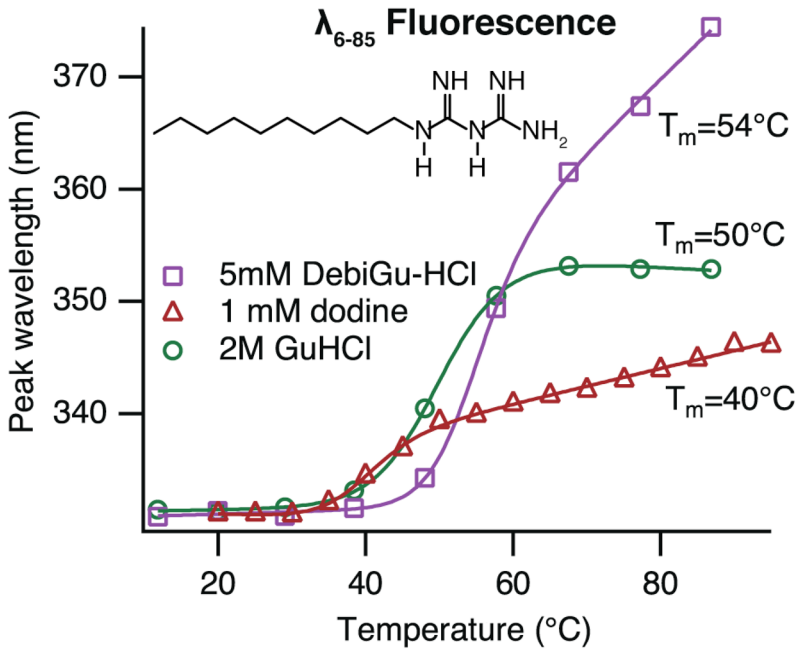

Figure 6.

$\lambda_{6\text{-}85}$ thermal denaturation monitored by fluorescence spectroscopy in the presence of 2 M guanidinium (green), 1 mM dodine (red), and 5 mM DebiGu (purple). Circles, squares and triangles represent experimental points; solid lines are thermodynamic fits to the data. Denaturation midpoints resulting from the fits to Equation 3 are shown. Inset shows the chemical structure of DebiGu (compare to the dodine structure in Figure 1a).

Table 1

Melting temperature of λ and WW domain with guanidinium and dodine.

Experiment	Parameter	No denaturant	Guanidinium	Dodine
λ Fluor	T_m (°C)	72±2	38±2 (2.5 M)	37±2 (1.65 mM)
	δg_1 (J/mol/K)	600±50	560±30	780±360
λ CD	T_m (°C)	71±2	42±2 (2.5 M)	-
	δg_1 (J/mol/K)	810±90	530±90	-
WW Fluor	T_m (°C)	74±2	54±2 (2.5 M)	69±2 (1 mM)
	δg_1 (J/mol/K)	400±30	290±120	520±50
WW CD	T_m (°C)	75±3	63±6 (2.0 M)	70±2 (1 mM)
	δg_1 (J/mol/K)	380±80	260±100	420±40